Using AI with the magnetic gradient tensor to map basement

D. Pratt[1], K. McKenzie[1], A. White[1]
1. Tensor Research, Australia, David.Pratt@tensor-research.com.au

BIOGRAPHY

David Pratt is a Director of Tensor Research. He holds a B.Sc. (Hons) and M.Sc. from the University of Sydney in Geology and Geophysics and a Ph.D. in Physics, University of Newcastle. His early career included the NSW Geological Survey, seismic processing company Digitech and Layton Geophysical Consultants. In 1979 he worked as a geophysical consultant and in 1984 he co-founded Encom Technology. He was Managing Director from 2001 until it was acquired by Pitney Bowes Business Insight in 2007. In 2010 he started Tensor Research with two colleagues to focus on advanced potential fields research. He received the ASEG's Grahame Sands Award in 2010.

SUMMARY

Most regional scale magnetic maps are dominated by the magnetic characteristics of steeply dipping basement units truncated by an unconformity surface. It is easy to demonstrate that 80 to 90% of each total magnetic field anomaly is contributed by this intersecting surface. We approach this problem by mapping the boundaries between contrasting magnetic units along each line in the magnetic survey using the full precision of the line data and 3D information from the magnetic gradient tensor. Additionally, we derive the azimuth of each boundary, depth to the unconformity and magnetic properties of the anomalous units. The segments are overlain on any image such as existing geological maps, satellite imagery, gravity or magnetic imagery to provide a new geological interpretation concept. This method provides a new way to interpret new and old magnetic surveys.

Eigenvector analysis of the magnetic tensor and normalised source strength (NSS) are combined with an artificial intelligence (AI) approach to estimate the basement properties. The method is applied to full tensor magnetic survey data or tensor data derived from FFT transformation of grid magnetic data. These data are used as input to the pre-trained AI process for calculation of depth, width, azimuth, magnetic susceptibility and magnetisation direction. The rock properties and depth information can be used for 3D visualisation of the unconformity and 2D mapping of the magnetic lithology of the unconformity surface.

Key words: AI, magnetic, tensor, mapping, basement.

INTRODUCTION

An AI approach requires a geological model concept that is well suited to automated interpretation. Our autonomous approach to geological mapping is based on three important concepts;

- The unconformity geological model,
- Geological attributes of the magnetic tensor,
- An AI approach to converting attributes to geology.

There are numerous tools available to assist geoscientists with the interpretation of aeromagnetic surveys ranging from specialised enhancement tools to full 3D modelling and inversion of the data. Enhancement methods are generally focussed on differentiating geological units in a 2D sense, while modelling and inversion require an underlying geological concept to provide appropriate constraints for building a 3D model.

We focus on the use of a geologic model to produce a new approach to geological mapping of the basement unconformity surface. This concept was first developed by Pratt et al. (2001) to build a starting 3D model of an isolated magnetic anomaly for seeding a 3D magnetic inversion.

Our understanding of the inherent information that can be derived from the magnetic tensor has extended our original concept to allow autonomous mapping of the unconformity with the aid of AI concepts. We use an expert system, artificial intelligence (AI) methodology for integrating the complex relationships between the quantitative geophysical methods and constraining geological principles (Pratt et al., 2019).

Unconformity Dominance

The dominant influence of the unconformity surface on measured magnetic anomalies is often ignored in large scale voxel inversions. A cursory review of most exploration and regional surveys will show the magnetic images are an excellent proxy for the geology at the unconformity surface. This dominance is illustrated in Figure 1 which shows that more than 90% of the total magnetic intensity anomaly is derived from the unconformity surface, with the remaining 10% distributed between the surface and the Curie point.

The model is a linear magnetic formation extending from the unconformity at 200 metres below the sensor to a depth of 10,000 metres. The base of the model was then raised to depths of 1,000, 500 and 200 metres and then inverted against the original 10,000 metre depth extent model data. The total magnetic intensity curves are shown in the middle track and the residual difference curves are shown in the top track at the same scale. The RMS difference between each of the models is shown to the left of each model.

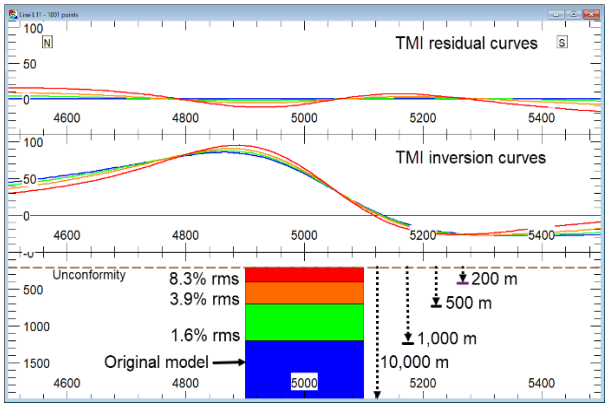


Figure 1. Illustration of the dominance of the unconformity. The four models are 200 m wide, 200 m below the sensor with depth extents of 200 m (red), 500 m (orange), 1000 m (green) and 10 km (blue) below the unconformity. The middle track shows the TMI curve in blue for the 10 km depth extent model and the inverted responses for the other three depth extents. The upper track shows the residual difference curves with rms values of 1.6%, 3.9% and 8.3% for the 1000 m, 500 m and 200 m depth extent models.

The implications of these results are used to support the robustness of the unconformity model concept behind the AI approach to continuous mapping.

FROM TENSOR TO GEOLOGY

The anomalous magnetic tensor is an abstract concept best imagined as a continuous change in curvature of the Earth's magnetic field. Direct measurement of the tensor in an airborne platform is now possible (Chwala et al., 2012, Stolz et al., 2017) and it can also be derived from a grid of the total magnetic intensity using Fourier transformation (Pratt et al., 2018).

Unlike TMI data, a single tensor measurement has inherent 3D properties that provide information about the geology on either side of the flight line. This insight leads us to the concept of using tensor line data to build a geological model that consists of one segment for each anomaly on every line in the survey (Figure 2).

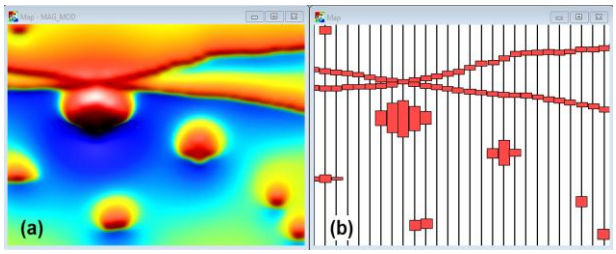


Figure 2. Colour image of the total magnetic intensity (a) and the segment model used to compute the response (b).

We explore here the geological properties that can be derived from the magnetic tensor without requiring inversion of one or more tensor measurements. The magnetic gradient tensor is defined in equation 1.

$$\Gamma = \begin{bmatrix} B_{xx} & B_{xy} & B_{xz} \\ B_{yx} & B_{yy} & B_{yz} \\ B_{zx} & B_{zy} & B_{zz} \end{bmatrix} = \begin{bmatrix} \frac{\partial B_x}{\partial x} & \frac{\partial B_x}{\partial y} & \frac{\partial B_x}{\partial z} \\ \frac{\partial B_y}{\partial x} & \frac{\partial B_y}{\partial y} & \frac{\partial B_y}{\partial z} \\ \frac{\partial B_z}{\partial x} & \frac{\partial B_z}{\partial y} & \frac{\partial B_z}{\partial z} \end{bmatrix} \quad (1)$$

Eigenvector decomposition of the symmetric tensor matrix produces a rotated and simplified version of the tensor ($\underline{\mathbf{\Lambda}}$) (Pedersen & Rasmussen, 1990, Clark 2012).

$$\underline{\mathbf{\Lambda}} = \begin{bmatrix} \lambda_1 & 0 & 0 \\ 0 & \lambda_2 & 0 \\ 0 & 0 & \lambda_3 \end{bmatrix} \quad (2)$$

where $\lambda_1 > \lambda_2 > \lambda_3$ are the eigenvalues of the magnetic gradient tensor.

Pedersen & Rasmussen (1990) also derive several parameters from the eigenvalues that are important for extracting useful geological characteristics from the target anomalies. The rotational invariants I1 and I2 are defined as;

$$I_1 = B_{xx}\,B_{yy} + B_{yy}\,B_{zz} + B_{xx}\,B_{zz} - B_{xy}^2 - B_{yz}^2 - B_{xz}^2\,, \quad (3)$$

$$I_2 = B_{xx}\,(B_{yy}B_{zz} - B_{yz}^2) + B_{xy}\,(B_{yz}B_{xz} - B_{xy}B_{zz}) + B_{xz}\,(B_{xy}B_{yz} - B_{xz}B_{yy})\,. \quad (4)$$

The dimensionality index is defined as:

$$I = -\left(\frac{(I_2/2)^2}{(I_1/3)^3}\right). \quad (5)$$

This parameter is very important because it can tell us if the target is pipe-like (~1) or has extended strike (~0). It provides the AI system with a numeric value that can separate pipes from dykes and a continuum in between. A pluton with an elliptic shape could have an I value of around 0.5 to 0.75. This one parameter helps provide important information for depth and magnetic susceptibility estimation.

If the dimensionality is low, then the source also has a strike or azimuth direction that can be computed from the tensor components (Pedersen & Rasmussen, 1990).

$$\tan(2\,\theta_s) = 2\,\frac{\left(B_{xy}\left(B_{xx} + B_{yy}\right) + B_{xz}B_{yz}\right)}{\left(B_{xx}^2 - B_{zz}^2 + B_{xz}^2 - B_{yz}^2\right)} \quad (6)$$

where, θ_s is the strike direction of the longer axis of the magnetic source.

Parameters derived from NSS

We only need to calculate the dimensionality index and strike direction at the centre of magnetisation rather than as continuous functions. Clark (2012) further developed

the concept of normalised source strength (NSS, μ), originally developed by Wilson (1985) as an important new parameter that could be derived from the magnetic gradient tensor (Equation 7).

$$\mu = \sqrt{(-\lambda_2^2 - \lambda_1\lambda_3)} \quad \text{where } \lambda_1 > \lambda_2 > \lambda_3 \qquad (7)$$

It has many special characteristics because it is semi-independent of the source magnetisation direction. The NSS parameter peaks over the centre of magnetisation for discrete bodies and along the central axis of elongate sources. For wide sources, NSS peaks over the edge and for narrower targets the maximum gradient point of the NSS anomaly profile define the outer limits of the high magnetisation zone.

We use Nelson's formulation (Nelson, 1988) to compute an estimate for the apparent magnetic susceptibility;

$$k = 0.625\, z\, T_{g0}\, /(B_{IGRF}(\sin^2 I_f + \cos^2 D_f)), \qquad (8)$$

where the total gradient is

$$T_{g0} = \sqrt{(B_{xx}^2 + B_{yy}^2 + B_{zz}^2)} \qquad (9)$$

and

z is the target depth below the sensor,
B_{IGRF} is the inducing field strength,
I_f is the magnetic field inclination,
D_f is the magnetic field declination.

A first order detection for remanence is determined by a sign reversal of the vertical gradient component B_{zz} or the first invariant I_1 at the centre of magnetisation.

Beike et al (2012), Clark (2014) and McKenzie (2019) show that the inclination ϕ of the magnetisation of a compact source (including a dipole, sphere, ellipsoid and vertical pipe) can be calculated from the tensor measurement over the centre of magnetisation using the following formula:

$$\phi = \cos^{-1}(\lambda_2/\mu) - \pi/2 \quad (0 \leq \phi \leq \pi) \qquad (10)$$

where λ_2 is the second eigenvalue and μ is the normalised source strength.

From the magnetic tensor over the centre of magnetisation and the NSS profile, we recover many geological attributes for each target anomaly;

- Segment style - pipe, elliptic pluton or dyke-like,
- Strike direction for elongate segments,
- Centre of magnetisation (origin),
- Apparent magnetic susceptibility,
- Magnetic reversals,
- Magnetisation inclination,
- Segment edges.

The tensor and segment model concept provide a foundation for anomaly detection and analysis of the attributes of the magnetic anomaly source. A complete model of the geology requires enough segments to provide a suitable source for every anomaly on every line in the survey where the anomaly amplitude exceeds a predetermined threshold.

AI EXPERT SYSTEM

All the parameters derived up to this point are considered hard facts that are based on geophysical theory and reproducible on any computer system. As interpreters, we use a lot of soft information as part of the process for converting geophysical data into a meaningful, geological/geophysical interpretation. We ultimately want to estimate the depth and magnetic properties of each segment and assess the quality of solutions that might be compromised by interference or limitations in the geophysical model. The AI expert system utilises the hard geophysical properties and soft information along with a suite of rules and iterative analysis to build a 3D segment geological model. The training of the system to build the rules and iteration procedures are implemented by an experienced interpreter.

We analyse both sides of every NSS anomaly (Figure 3) and collect information such as;

- Peak and trough locations,
- Inflection point locations,
- Curvature point locations,
- Interference,
- Characteristic amplitudes,
- Characteristic widths,
- Characteristic ratios.

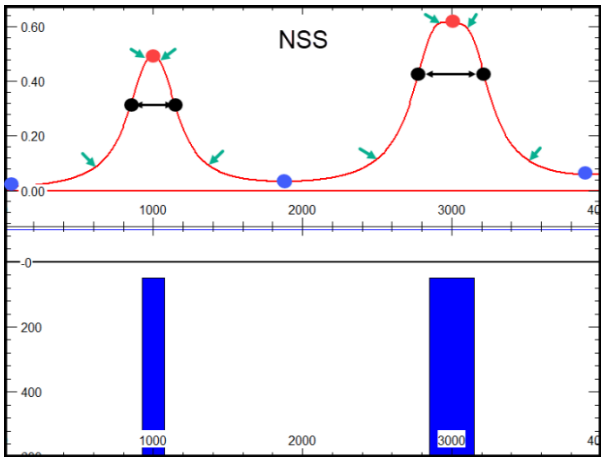


Figure 3. The NSS response over two magnetic bodies 150m below the sensor and widths of 150 and 300 metres. The field inclination is -60 degrees and declination 10 degrees north. The peaks (red dots), troughs (blue dots), inflection points (black dots) and curvature points (green arrows) represent the characteristic points on the NSS curve.

The ratio of depth to width (DW) is an important factor for improving the quality of depth interpretation and as part of the training of the AI system we have developed a set of shape tests to detect ratios in the range 1.0 < DW < 2.0. The width classification information is then used to correct the initial body width which is based on the location of the inflection points.

The inflection and half-slope curvature points (Peters, 1949) of the NSS anomaly curve form the foundation for the estimation of an initial depth value. This initial value is then corrected based on the depth-to-width classification and strike azimuth relative to the line direction. The strike azimuth correction is only applied to low dimensionality (*I*) anomalies.

A preliminary depth estimate is computed for each side of the NSS profile using the characteristic curvature. A strike correction is applied first to the depth estimate and then the AI system uses input from the dimensionality index (*I*), segment width, anomaly type classification and interference to correct the depth using the training information determined from trial geological models. The magnetic susceptibility estimate is then calculated using the depth and total gradient data (Equations 8 and 9) and refined using the training information.

MODEL TESTS

Many surveys were simulated over varying geological models to provide both insights into parameter sensitivity and training data for calibration of the AI system. Figure 4 shows a plot of isolated tabular models with finite strike length, variable orientation and variable magnetic susceptibilities designed to test the azimuth calculations. Azimuth-oriented, coloured segments are posted over the original models (black outline) that were used to generate the magnetic tensor data. The symbols are colour coded by the estimated segment depth with azimuth annotations beside the symbols. If the end segments are excluded, the estimated azimuth results are all within 1 to 2 degrees of the model orientations.

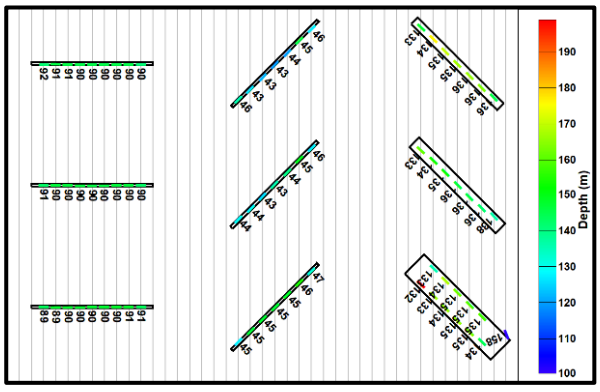


Figure 4. A symbol plot of individual AI segment solutions using the azimuth to control symbol rotation, depth to modulate colour and the annotations show the computed azimuth value.

Different logic is required to recognise and manage the end members of a string of segments. Work on this logic is part of a parallel research project that chains segments together from adjacent lines for use in the assessment of property variance along the chain.

While there is a strong impression of coherence in the distribution of segments, they have been located and oriented on an individual basis with no knowledge of segments on adjacent flight lines. An example of the effect can be seen in Figure 5 which shows the depth results for a series of circular and elliptic shaped intrusive pipes, all at a depth of 150 metres below the sensor. The central segments for each pipe are within 10 metres of the true depth, but for the elongate pipes, the depths deteriorate towards the ends due to the longer anomaly wavelengths near the ends. This decrease in accuracy can be ameliorated by using AI principles or inversion.

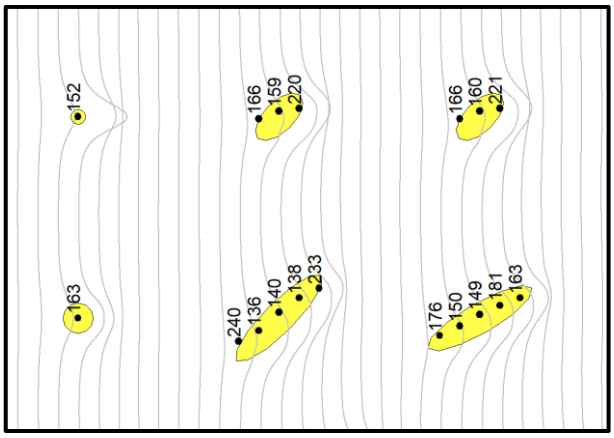


Figure 5. A stacked profile map of the NSS parameter posted over the original pipe models and AI derived segments (black dot locations) with individually computed depth estimates.

CASE HISTORY

The AI system was applied to a recent data subset from the South Australian PACE Copper program over the Gawler Craton, Torrens sheet. The total field magnetic and radiometric survey was flown in 2017 at 200 metre line spacing and 60 metre terrain clearance by Sander Geophysics Limited (Bates and Dennis, 2018). A geophysical report on the image processing and depth interpretation of the survey results is presented by Foss et al., (2018).

The total magnetic intensity image for the Torrens survey area is shown in Figure 6. The north-west trending Gairdner Dyke swarm disturbs the high amplitude anomalies associated with the deeper magnetic basement. The magnetic tensor data was computed by FFT transformation of the TMI data using ModelVision (Pratt et al., 2018). The grid data was then resampled back on to the original flight lines in preparation for the AI processing.

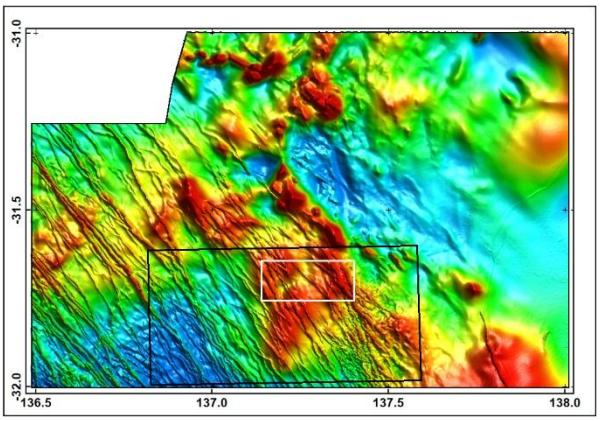


Figure 6. A total magnetic intensity image of the total magnetic intensity grid supplied by the South Australian Geological Survey. The black rectangle shows the location of data used in the case history and the white rectangle covers the sub-area shown in Figure 7.

Figure 7 presents some of the interpreted attributes after the AI processing of a subset of the study area results, overlain on a monochrome image of the total magnetic intensity. Approximately 50 attributes have been computed by the AI system at this stage of processing and many are suitable for display as symbols with attributes such as size, colour, azimuth and text. In Figure 7 we have chosen to use black dots where the size is modulated by the AI system estimate of depth confidence. The text annotation is used for the estimated depth below the ground surface. Beneath the symbol, a model representation of the upper surface of each segment is shown and colour coded by the magnetic susceptibility.

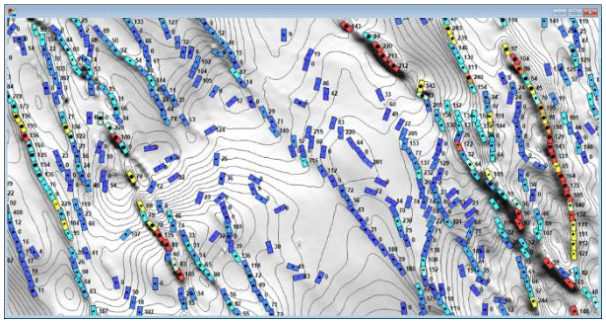


Figure 7. A subset of the study area posted over a monochrome image and contours of the total magnetic intensity grid. Individual segment models were derived from the anomaly attributes and are oriented according to the tensor-derived azimuth and colour coded by magnetic susceptibility. The depth annotations show depth (m) below the ground surface and the associated black dot varies in size according to the AI assessment of depth quality.

At this point in the process, the segments have been generated independently of segments from adjacent lines, however the process demonstrates that there is considerable coherence in the spatial relationships. The model segments have a strike direction that was derived directly from the tensor (Equation 6) and are colour coded by the estimated magnetic susceptibility (Equation 8). The depth confidence (black dot size) provides a useful guide on which depths to use during interpretation.

These preliminary results suggest the existence of four unconformity surfaces;

- Sub-crop or surficial 0 to ~50 metres, generally lack spatial coherence,
- Gairdner Dykes 50 to 100 metres, low susceptibility,
- Gairdner Dykes 100 to 200 metres
- Basement >250 - 300 metres (not shown here).

Figure 8 shows the model segments for the whole study area overlain on a monochrome image of the total magnetic intensity grid, but without the depth annotations. The coherence of the individual azimuth-oriented model segments is evident and enhances the interpreter's ability to absorb the underlying geological information.

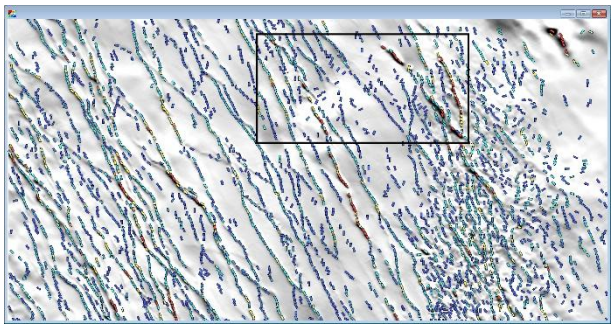


Figure 8. Model segments for the complete study area are posted over a monochrome image of the total magnetic intensity grid. Individual segment models were derived from the anomaly attributes and are oriented according to the tensor-derived azimuth and colour coded by magnetic susceptibility. The black rectangle shows the sub-area covered by Figure 7.

Figure 9 shows one of many possible display styles where attributes are used to modulate the size and colour of filled circles. In this case, the colour represents magnetic susceptibility and the size is controlled by the susceptibility-thickness product. Since it is not possible to estimate the thickness of the dykes, the susceptibility-thickness product becomes a useful diagnostic parameter. Other parameters include width, magnetisation inclination, magnetisation declination, apparent magnetisation departure angle, anomaly reversal, pipe classification, dimensionality, anomaly amplitude, interference and many others.

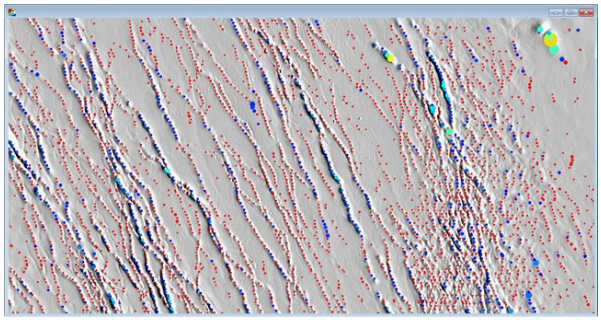


Figure 9. Coloured symbols are modulated by magnetic susceptibility from blue (low) to high (red) and the symbol size is modulated by the susceptibility-thickness product.

CONCLUSIONS

We have demonstrated that is possible to use the inherent 3D information in the magnetic gradient tensor along with the higher resolution of flight line data to build a 3D magnetic model of one or more unconformity surfaces. The problem is simplified by using a single segment for every anomaly in every line in the survey where the segment strike length is equal to the line spacing.

The AI expert system plays an important role by applying geological principles to the assessment and refinement of every segment in the survey. The additional information produced by the AI system provides the interpreter with important shape, property and quality attributes which make the process of interpretation more robust. We believe that neural network AI methods also have a role to play in improving some of the classification parameters that are used by the expert system. Unlike neural networks, the system rules are developed by an expert interpreter and hard coded within the expert system algorithms. The pre-conditioning of the input hard and soft parameters to ensure they are closely correlated with the target properties is an important component of the expert system approach.

The AI process assumes that all anomalies are truncated by an unconformity surface which is a practical assumption for many airborne surveys. It does not attempt to consider continuous property variations except at the scale of the flight line spacing.

This research is the first stage of a multi-stage AI process designed to produce coherent, quantifiable 3D magnetic lithology models at a resolution that reflects the detail present in the original survey. These results provide the foundation for exploring the links between adjacent segments, lateral continuity along segment chains, equivalent source joint inversion of the magnetic gradient tensor, micro-adjustment of individual segments based on joint inversion and magnetisation property recovery through inversion.

ACKNOWLEDGMENTS

We would like to acknowledge the input of Anglo Operations and De Beers for their encouragement and partial support for the development of a new way of interpreting full tensor magnetic data.

REFERENCES

Bates,M., and Dennis, J., 2018, PACE Gawler Craton Airborne Geophysical Survey Program: Block 3B – Torrens, SGL Technical Report (unpublished) 218 pages

Beike, M., Clark, D.A., Austin, J.R. & Foss, C.A. 2012, Estimating source location using normalized magnetic source strength calculated from magnetic gradient tensor data: Geophysics, 77, (6), J23-J37.

Chwala, A., Stolz, R., Zakosarenko, V., Fritzsch, L., Schultz, M., Rompel, A., Polome, L., Meyer, M. and Meyer, H.G. 2012, Full Tensor SQUID Gradiometer for airborne exploration. Extended Abstracts, 22nd International Geophysical Conference and Exhibition, 26-29 February 2012 - Brisbane, Australia.

Clark, D.A., 2012, New methods for interpretation of magnetic vector and gradient tensor data I: eigenvector analysis and the normalised source strength: Exploration Geophysics, 43, 267-282.

Foss, C.A., Gouthas, G., Fabris, A., Werner, M., Katona, L., Hutchens, M. & Reed, G. 2018, Gawler Craton Airborne Geophysical Survey Region 3B, Torrens – Enhanced geophysical imagery and magnetic source depth models. Report Book 2018/00038, Government of South Australia, 76p.

Pedersen, L.B. & Rasmussen, T.M., 1990, The gradient tensor of potential field anomalies: Geophysics, 55 (12), 1558-1566.

Peters, L.J. 1949, The direct approach to magnetic interpretation and its practical application. Geophysics, 14(3), 290-320.

Pratt, D.A., McKenzie, K.B., White, A.S., Foss, C.A., Shamin, A. and Shi, Z. 2001, A User Guided Expert System Approach to 3D Interpretation of Magnetic Anomalies. Extended Abstracts, ASEG 15th Geophysical Conference and Exhibition, August 2001, Brisbane.

Pratt, D.A., 2013, The potential of remote remanence estimation (RRE) for kimberlite exploration – A case history from the Thomson Fold Belt. Extended Abstracts, 23rd International Geophysical Conference and Exhibition, 11-14 August 2013 - Melbourne, Australia.

Pratt, D.A., McKenzie, K.B. and White, A.S., 2014, Remote remanence estimation (RRE). Exploration Geophysics, 45(4), 314-323.

Pratt, D.A., Parfrey, K., White, A.S. & McKenzie, K.B. 2018, ModelVision v16.0 User Guide, pub. Tensor Research, 599p.

Pratt, D.A., McKenzie, K.B. and White, A.S., 2019, An AI approach to using magnetic gradient tensor analysis for quick depth and property estimation. Extended Abstracts, AEGC 2019: From Data to Discovery – Perth, Australia.

Stolz, R., Zakisarenko,V., Schmelz, M., Schiffler, M., Chwala, A., Meyer, M. and Meyer, H.G. 2017, SQUIDs in exploration: the past, present and future. Extended Abstracts - 15th SAGA Biennial Conference & Exhibition.